21st Australasian Fluid Mechanics Conference
Adelaide, Australia
10-13 December 2018

A numerical study of pulsatile microflows for embryo culturing in microfluidics

Jiaming Shi[1], Jun Dong[1], Huaying Chen[1], Yijuan Sun[2], Xiaoxi Sun[2,3] and Yonggang Zhu[1,4]

[1]School of Mechanical Engineering and Automation, Harbin Institute of Technology (Shenzhen), Shenzhen, China

[2]Shanghai Ji Ai Genetics & IVF Institute, Obstetrics & Gynecology Hospital, Fudan University, Shanghai, 200011, China

[3]Shanghai Key Laboratory of Female Reproductive Endocrine Raleted Diseases

[4]School of Science, RMIT University, Melbourne, VIC 3001, Australia

Abstract

An embryo is subject to dynamic mechanical stimuli exerted by a fallopian tube before implantation, which may include shear stress, compression and friction. The mechanical microenvironment plays vital role in the early development of an embryo. In addition, the oviduct fluid is flowing in a pulsatile manner with a certain frequency, rather than constant. The purpose of this study is to simulate the mechanical stimulation of the oviduct fluid on an embryo, in order to model the mechanical microenvironment of an embryo in vitro. In this simulation, a rigid bead with the diameter of 300 microns was used to represent the embryo placed in three different sites on the floor of a microchamber with the diameter of 1 mm. A pulsatile flow with the average velocity of $V=2.4\times\sin(2\pi t/7.4) + 2.5$ (μm/s) was set up at the inlet port. The numerical study shows that the shear stress is also change with time and it's the same trend with velocity. In addition, the maximum shear stress appears at the junction of the culture dish and the outlet channel and it is 2.7×10^{-2} dyn/cm^2, which is close to the shear stress experienced by mouse embryos in the fallopian tubes.

1. Introduction

Since the first in-vitro development of mouse zygote in oviduct tissue in 1941 [16], significant research and development effort has been made in this field to optimise the in-vitro culture conditions of embryos. The ex-vivo culture of embryos is usually performed in stationary media such as tubes or droplets [5,22,23]. However, embryos in vivo experience dynamic mechanical stimulation [9] and biochemical conditions [11] when it traverses the fallopian tube. The fallopian tube exerts a solid mechanical force on the embryo [1,2], these in vivo mechanical stimuli play an important role in the embryo development since they can alter the biochemical microenvironment around the embryo and facilitate the exchange of gases and biomolecules. The importance of microenvironment, embryo handling and culturing was reported as early as the 1970s [26]. Recently, adding a micro-well at the bottom of the dish [14,24] has been proven to improve embryonic development, possibly by affecting the culture microenvironment such as providing the appropriate nutrient supplementation and dilution of certain toxic metabolic products. In addition, an oocyte/embryo may undergo twenty times of manual manipulation during in vitro culture [25]. The manipulation directly results in a rapid variation of mechanical stress, temperature, gas concentration and pH. Therefore, gametes and embryos may be exposed to an environment where pH, osmotic pressure and mechanical stress are constantly changing, which may have negative effect on the development of the embryo.

According to the US Centres for Disease Control and Prevention, the birth rate of in-vitro fertilization (IVF) in the United States in 2015 was only about 40% [7], and it was even lower for patients over 38 years old. Currently, all in vitro culture methods employed in IVF clinics are not a substitute for the fallopian tubes in promoting embryo development. No system can produce embryos of the same quality as developed in vivo, probably due to the inability of mimicing the in vivo environment. There are many differences between culture conditions of embryos in vitro and in vivo, including develop mental speed, metabolic capacity, lipid concentration, gene expression, frost resistance, and embryo mortality after metastasis [3,12,15,19,20,22,27]. Therefore, it is important to generate in vitro culture environment which truly mimics the in vivo ones to improve the success rate of IVF.

In recent years, significant progress has been made in developing technologies enabling the mimic of the in-vivo microenvironment of an embryo. Most of them are microfluidics based technologies, e.g., (a) shear stress by tubal fluid flow; (b) compression by peristaltic tubal wall movement; (c) buoyancy; and (d) kinetic friction forces between the embryo and cilia. For example, the transport and retention of individual embryo have been performed using microfluidic chips [10]. A uterine chip was employed to simulate the human uterus environment [8, 29]. In addition, in order to better simulate the in vivo environment and improve embryonic development, researchers have tried many other microfluidic technologies, such as mechanical vibration, rotation and flow rate control [13,18,21], to provide a dynamic culture environment for embryos. The purpose of this study is to calculate the shear stress applied on the embryo model at different position of the microchamber with a pulsatile flow, and to provide theoretical basis for future embryo culturing technique developments.

2. Materials and methods

2.1 Model geometry

The model consists of a rectangular inlet channel, a cylindrical culture chamber and an outlet channel (figure 1a). The sizes of the inlet and outlet channels are 500 μm × 500 μm and 500 μm × 100μm (h × w), respectively, and the height of the cylindrical culture chamber is 500 μm and the diameter is 1000 μm. A spherical bead with a diameter of 300 μm was used to model an embryo. The coordinate system is shown in figure 1a schematically, and the origin is at the center of cylindrical culture chamber.

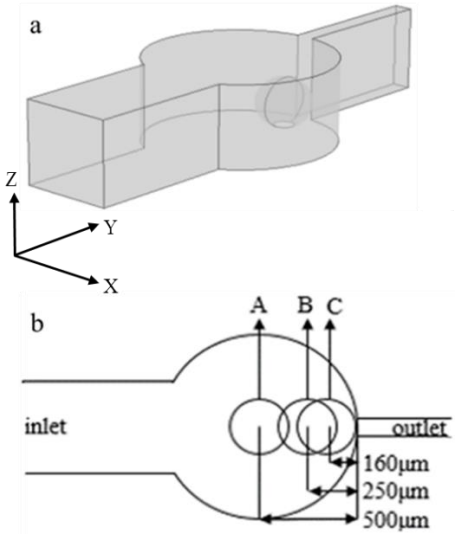

Figure 1. (a) Geometry of the microfluidic model, (b) positions of the bead in the culture chamber.

2.2 Governing equations

In this simulation, we assume a flow of an incompressible Newtonian fluid. In this case, the conservation equation of mass and momentum are shown as follows:

$$\nabla \cdot \vec{V} = 0 \tag{1}$$

$$\frac{\partial \vec{V}}{\partial t} + \vec{V} \cdot \nabla \vec{V} = -\frac{1}{\rho} \nabla P + \frac{\mu}{\rho} \Delta \vec{V} \tag{2}$$

where ρ is the fluid density, $\vec{V}$ is the fluid velocity, μ is the dynamic viscosity and P is the pressure.

2.3 Boundary conditions

The 3D model was created in Creo (PTC Inc.) first and then imported into COMSOL Multiphysics (COMSOL Inc.) for meshing and simulating. The fluid flow in the model domain was assumed to be laminar and the flow field was solved in time dependent condition. The inlet velocity was time dependent as a sinusoidal function, as shown in figure 2, which is close to the periodic physiological conditions of human body. At the outlet, a constant atmosphere pressure was assumed. A no-slip boundary condition was applied at all wall boundaries (i.e. the fluid has zero velocity relative to the wall).

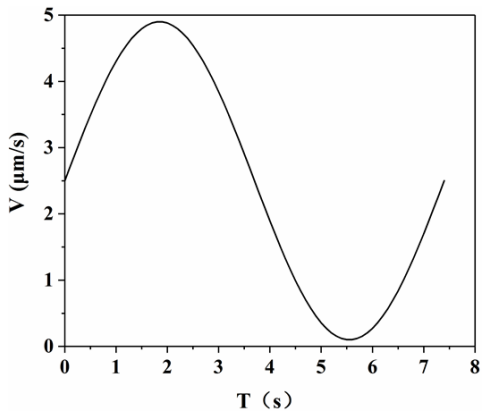

Figure 2. The inlet velocity as a function of time.

2.4 Meshing

Tetrahedral meshes, triangular meshes and boundary layer meshes were employed for automatic meshing. Grid independence validation was performed, where 0.14 million, 0.42 million, 1.02 million and 2.64 million elements were used for the numerical studies. It is found that when the number of elements was over 0.42 million, the flow velocity/shear rate of the same region did not vary significantly. Therefore, the models with 0.42 million elements were employed for all studies in order to save the computation time.

2.5 Shear stress study

The shear stress of the bead at different positions in the chip is calculated in order to found out which position is more close to the shear stress experienced by mouse embryos in the oviduct. Three positions (figure 1b) which are 160μm, 250μm and 500μm away from the joint between the culture chamber and the outlet channel were selected for this study.

3. Results and discussion

3.1 Flow fields

The streamlines of the flow are shown in figure 3 for three different bead positions. In order to more clearly describe the difference of flow fields between the three cases, we took a line directly above each bead (figure 4a) and plotted the velocity distribution (figure 4c). From this figure, we can see that the fluid velocity gradually increases from position A to position C, and the maximum velocities above the bead at positions A, B and C are 4.9 μm/s, 9.2 μm/s and 19.9 μm/s, respectively. Due to the sudden decrease of the cross section at the joint between the culture chamber and the outlet channel, the maximum values at positions B and C appear on the regions behind (downstream side) the bead rather than above the bead as that for bead at position A, and the maximum values are 43 μm/s and 62 μm/s for positions B and C, respectively.

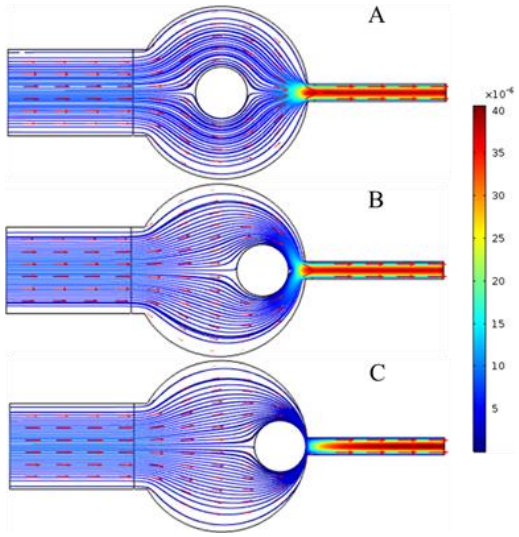

Figure 3. Streamline distribution on the cross section of bead at the three different positions at the peak velocity moment. The colour bar indicates the magnitude of flow velocity.

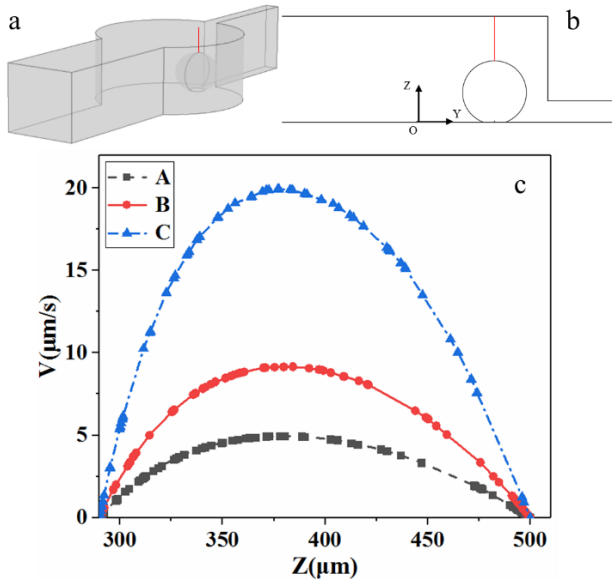

Figure 4. Velocity along the centerline of the bead surface for the three different bean positions. Z is measured from the bottom of the channel (or bead).

3.2 Shear rate on the surface of the bead at different positions

The distribution of shear rate on the bead surface at different locations is shown in figure 5 (In the figure, the left side of the bead is towards inlet). The maximum shear rate on the surface of the bead at these three positions is 0.15 s^{-1},0.71 s^{-1} and 2.68 s^{-1}, respectively (figure 5). Figure 6a shows the contour of shear rate on the bead surface projected from the outlet port to the inlet port direction. In order to more clearly show the shear rate on the surface of the beads, the shear rates along two lines on the bead surface are shown in figure 6b (1-3). One line is along the centre of the bead and the other is 50 μm from bead centre. Figure 6b reveals that the shear rate varies significantly over on the bead surface and the maximum shear rate of position A appears at the top of the bead, while the maximum shear rate of positions B and C appears at the downstream sides of the beads, which is consistent with the velocity distribution. Figure 6b-4 shows the comparison of shear rate along the centreline (A2, B2, C2) of the bead when placed at three different locations. The position of the bead has a great influence on the shear rate. The value increases from position A to position C, and the value of position C is 20 times greater than position A.

The shear stress τ is directly dependent on the shear rate $\dot{\gamma}$, i.e.,

$$\tau = \mu\dot{\gamma}\,. \tag{3}$$

The shear rate is defined as: [6]

$$\dot{\gamma} = (\nabla\vec{u} + (\nabla\vec{u})^T) \tag{4}$$

It is found that the shear stress of the bead at position C is closest to the shear stress of embryo in fallopian tube (Table 1). Then we draw the relationship between the shear stress and the time at position C (figure 7), and we found that the variation of shear rate with time is similar to velocity.

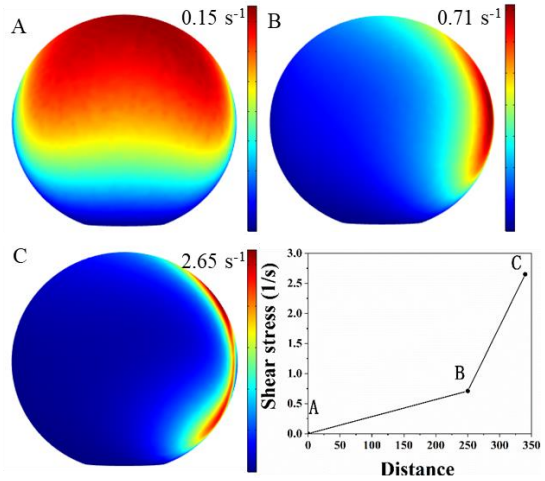

Figure 5. Side view of shear rate distribution at peak velocity on the surface of the bead at location A, B and C, respectively.

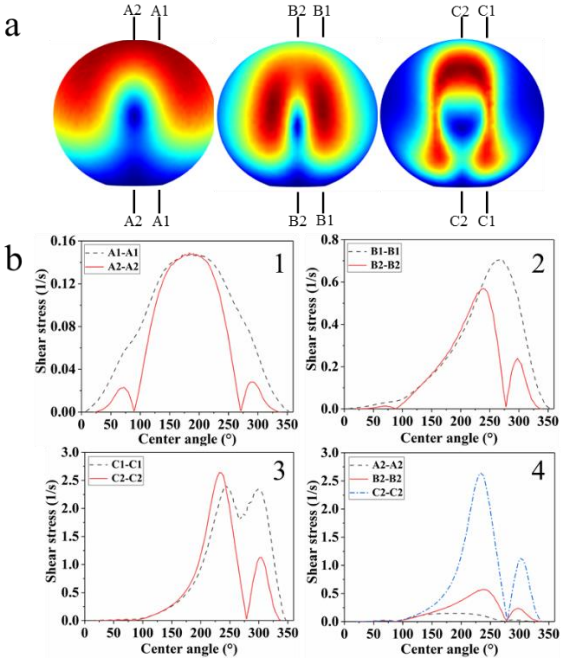

Figure 6. Backview of the shear rate distribution on bead surface. (a) contour plot (b) distributions along the centreline (A2, B2, C2) and a line offset by 50 μm from centreline (A1, B1, C1).

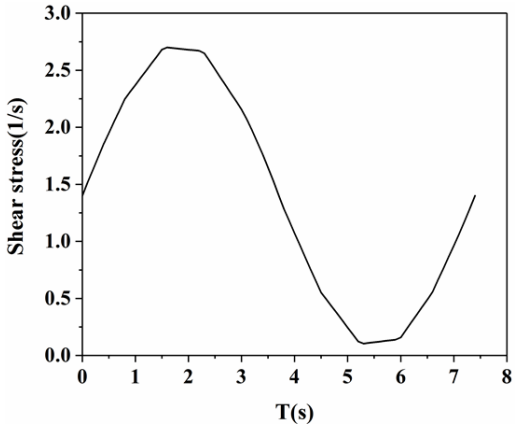

Figure 7. Variation of shear rate with time at position C.

	Velocity of medium (μm/s)	Shear stress (dyn/cm^2)
Position A	0-43	0-1.5 ×10^{-3}
Position B	0-43	0-7.1 ×10^{-3}
Position C	0-62	0-2.7 ×10^{-2}
In extirpated mouse oviduct	0-100	0-3 ×10^{-2}

Table 1 Comparison between fluid velocity, shear stress in the chip and in the oviduct.

4. Conclusions

In this paper, we have studied the shear stress on beads placed at three different sites in a microchamber with a pulsatile flow. It is found that the shear stress on the bead varied greatly as the change of the positions in the centre line of a microchamber along the flow. The shear rate also varies with time due to the velocity variation of the pulsative flow. The maximum shear stress experienced by the bead in this study is about 0-2.68 ×10^{-2} dyn/cm^2, which is close to the shear stress in the fallopian tube. Therefore, through this simulation we provide a model for embryo culture which can mimic the oviduct environment, the fluid velocity in the model and the shear stress of the beads is similar to the oviduct situation. So the implantation rate of embryo cultured with this chip model may be improved, and we will conduct experimental verification in future research.

Acknowledgments

The start-up financial support for Prof. Yonggang Zhu from Harbin Institute of Technology and Shenzhen Science and Technology Innovation Commission is gratefully acknowledged.

Reference

[1] Anand, S. and S.K. Guha, *Mechanics of transport of ovum in oviduct.* Med. & Biol. Eng. & Comput., 1978. **16**: p. 256-261.

[2] Blake, J.R., P.G. Vann, and H. Winet, *A model of ovum transport.* J. theor. Biol., 1983. **102**: p. 145-166.

[3] Boni, R., et al., *Intercellular communication in in vivoand in vitro-produced bovine embryos.* Biol Reprod, 1999. **61**: p. 1050-1055.

[4] Bourdage, R.J. and S.A. Halbert, *In vivo recording of oviductal contractions in rabbits during the periovulatory period.* Am J Physiol 1980. **239**: p. 332-336.

[5] Brison, D.R., et al., *Identification of viable embryos in IVF by non-invasive measurement of amino acid turnover.* Hum Reprod, 2004. **19**(10): p. 2319-24.

[6] "COMSOL Multiphysics Reference Manual, version 5.3", COMSOL, Inc, www.comsol.com.

[7] CDC, 2015 Assisted reproductive technology national summary report. 2017, Centers for Disease Control and Prevention, American Society for Reproductive Medicine, Society for Assisted Reproductive Technology: Atlanta, USA.

[8] Chang, K.-W., et al., *Womb-on-a-chip biomimetic system for improved embryo culture and development.* Sensors and Actuators B: Chemical, 2016. **226**: p. 218-226.

[9] Fauci, L.J. and R. Dillon, *Biofluidmechanics of reproduction.* Annu Rev Fluid Mech, 2006. **38**: p. 371-394.

[10] Glasgow, I.K., et al., *Individual Embryo Transport and Retention on a Chip. Springer Netherlands.* Springer Netherlands, 1998: p. 199-202.

[11] Hardy, K. and S. Spanos, *Growth factor expression and function in the human and mouse preimplantation embryo.* J Endocrinol, 2002. **172**(2): p. 221-236.

[12] Hasler, J.F., *In vitro culture of bovine embryos in Menezos B2 medium with or without coculture and serum the normalcy of pregnancies and calves resulting from transferred embryos.* Anim Reprod Sci, 2000. **60-61**: p. 81-91.

[13] Heo, Y.S., et al., *Real time culture and analysis of embryo metabolism using a microfluidic device with deformation based actuation.* Lab Chip, 2012. **12**: p. 2240-2246

[14] Hoelker, M., et al., *Effect of the microenvironment and embryo density on developmental characteristics and gene expression profile of bovine preimplantative embryos cultured in vitro.* Reproduction, 2009. **137**(3): p. 415-25.

[15] Khurana, N.K. and H. Niemann, *Energy metabolism in preimplantation bovine embryos derived in vitro or in vivo.* Biol Reprod, 2000. **62**: p. 847-856.

[16] Kuhl, W., *Untersuchungen uber die cytodynamik der furchung und fruhentwicklung des eis der weissen maus.* Abb Senchenb Naturforsch Ges 1941. **456**: p. 1-17.

[17] Matsuura, K., et al., *Improved development of mouse and human embryos using a tilting embryo culture system.* Reprod Biomed Online, 2010. **20**(3): p. 358-64.

[18] Mizobe, Y., M. Yoshida, and K. Miyosh, *Enhancement of cytoplasmic maturation of in vitro-matured pig oocytes by mechanical vibration.* J Reprod Dev, 2010. **56**(2): p. 285-290.

[19] Niemann, H., et al., *Gene expression patterns in bovine in vitro-produced and nuclear transfer-derived embryos and their implications for early development.* Cloning Stem Cells 2002. **4**: p. 29-38.

[20] Rubessa, M., et al., *Effect of energy source during culture on in vitro embryo development, resistance to cryopreservation and sex ratio.* Theriogenology, 2011. **76**(7): p. 1347-55.

[21] Smith, G.D., S. Takayama, and J.E. Swain, *Rethinking in vitro embryo culture: new developments in culture platforms and potential to improve assisted reproductive technologies.* Biol Reprod, 2012. **86**(3).

[22] Thompson, J.G., *In vitro culture and embryo metabolism of cattle and sheep embryos—a decade of achievement.* Anim Reprod Sci, 2000. **60-61**: p. 263-275.

[23] Thompson, J.G., *Culture without the petri-dish.* Theriogenology, 2007. **67**(1): p. 16-20.

[24] Vajta, G., et al., *New method for culture of zona-included or zona-free embryos: The Well of the Well (WOW) system.* Mol Reprod Dev, 2000(55): p. 256-264.

[25] Wheeler, M.B. and M. Rubessa, *Integration of microfluidics in animal in vitro embryo production.* Mol Hum Reprod, 2017. **23**(4): p. 248-256.

[26] Willadsen, S.M., *A method for culture of micro-manipulated sheep embryos and its use to produce monozygotic twins.* Nature, 1979. **277**(5694): p. 298-300.

[27] Wrenzycki, C., et al., *Expression of the gap junction gene connexin43 (Cx43) in preimplantation bovine embryos derived in vitro or in vivo.* Reprod Fertil Dev, 1996. **108**: p. 17-14.

[28] Xie, Y.F., et al., *Shear stress induces preimplantation embryo death that is delayed by the zona pellucida and associated with stress-activated protein kinase-mediated apoptosis.* Biol Reprod, 2006. **75**: p. 45–55.

[29] Xu, H. and Y. Inagaki, *A more womb-like chip for IVF was born in Japan.* BioSci Trends, 2007. **3**: p. 117-118.